Sleep Medicine 62 (2019) 53–58

Contents lists available at ScienceDirect

Sleep Medicine

journal homepage: www.elsevier.com/locate/sleep

Original Article

Small-world properties of the whole-brain functional networks in patients with obstructive sleep apnea-hypopnea syndrome

Yaqing Huang [a, 1], Yuting Liu [a, 1], Dadi Zhao [b, c], Bin Liu [d], Huixin Zhang [d], Zhichun Huang [d], Ben Babourina-Brooks [b, c], Andrew C. Peet [b, c], Lingling Zhang [e], Yuan Feng [f], Ting Cheng [g], Ming Yang [a, *], Yu Sun [b, c, h, **]

[a] Children's Hospital of Nanjing Medical University, Nanjing 210008, China
[b] Institute of Cancer and Genomic Sciences, University of Birmingham, Birmingham, UK
[c] Institute of Child Health, Birmingham Children's Hospital NHS Foundation Trust, Birmingham, UK
[d] The Affiliated Zhongda Hospital of Southeast University Medical School, Nanjing 210008, China
[e] The Second Affiliated Hospital of Soochow University, Suzhou 215000, China
[f] The Affiliated Nanjing First Hospital of Nanjing Medical University, Nanjing 210029, China
[g] The Affiliated Jiangyin Hospital of Southeast University Medical School, Wuxi 214400, China
[h] School of Biological Science and Medical Engineering, Southeast University, Nanjing 210018, China

ARTICLE INFO

Article history:
Received 10 May 2018
Received in revised form
3 August 2018
Accepted 27 August 2018
Available online 12 December 2018

Keywords:
Obstructive sleep apnea-hypopnea syndrome (OSAHS)
Magnetic resonance imaging
Brain's functional network
Small-world

ABSTRACT

Objective: To explore the small-world properties of brain functional networks in patients with obstructive sleep apnea–hypopnea syndrome (OSAHS) to aid diagnosis.
Methods: A total of 29 OSAHS patients and 26 matched healthy volunteers were scanned with blood oxygen level–dependent functional magnetic resonance imaging (BOLD-fMRI) separately, and the whole brain was divided into 90 districts via automated anatomical labeling. The matrix Z was then built through a Fisher Z transformation. Two-sample t tests were applied to evaluate the changes in small-world properties in OSAHS patients compared to the control group. The properties included E_{global}, E_{local}, and small-world parameters L_p, C_p, γ, λ, and σ.
Results: Both groups satisfied the small-world properties ($\sigma > 1$) within the sparsity range of 0.1–0.2. However, compared with the control group, the OSAHS group performed significantly lower in C_p, E_{local}, and E_{global} ($p < 0.05$) and higher in L_p ($p < 0.05$). The γ, σ, and λ values were not significantly different between the two groups.
Conclusion: Both healthy and OSAHS patients exhibited small-world properties in functional networks, but a subset of these small-world properties in OSAHS patients performed differently. These changes will not only provide a new perspective for pathophysiological mechanisms of OSAHS but will also help in understanding the disease in terms of whole-brain functional networks.

1. Introduction

As the most common type of sleep apnea in adults, obstructive sleep apnea–hypopnea syndrome (OSAHS) has serious influence on patients' quality of life. OSAHS is characterized by repeated episodes of complete or partial upper airway obstruction during sleep, accompanied by intermittent hypoxemia, snoring, and sleep fragmentation [1]. The corresponding outcome of hypoxemia (eg, recurrent hypopnea, even apnea), may cause sleepiness during the day. Moreover, excessive sleepiness has an impact on people's quality of life, as well as indirectly increasing the incidence of accidents. Several of these OSAHS features were correlated with the severity of the disorder [2–9]. Recurrent upper airway obstruction during sleep led to repeat apneas accompanied by oxygen desaturation and arousal from sleep. The most common complaint is the excessive day time sleepiness (EDS) [10]. A reduction in pO_2 and pH and an increase in pCO_2 have serious effects on the body, including

* Corresponding author. Children's Hospital of Nanjing Medical University, Nanjing 210008, China. Fax: +86 25 83304239.
** Corresponding author. School of Biological Science and Medical Engineering, Southeast University, Nanjing 210018, China. Fax: +86 25 83792349.
E-mail addresses: yangming19710217@163.com (M. Yang), sunyu@seu.edu.cn (Y. Sun).
[1] Yaqing Huang and Yuting Liu contributed equally to this work.

https://doi.org/10.1016/j.sleep.2018.08.037

the heart, lungs, and brain, which could result in sudden death during sleep in rare cases. Due to the serious effects on patient health and quality of life, a further understanding of OSAHS and measuring the effects on the brain are important.

Resting state functional magnetic resonance imaging (fMRI) has the advantages of its relatively simple task design. It can provide dynamic repeated observations noninvasively without a radiation dose. It can also provide meaningful data to help in the comprehension of the anatomy and function of the upper airway in OSAHS patients [11]. It has become a major tool for exploring regional brain function.

Recently, magnetic resonance imaging (MRI)–based graph theory has been used to typify the topological properties in brain networks [12], which is modeled as a graph with the nodes and the edges corresponding to the brain regions and the interregional connectivity, respectively. Path length (L_p) is short in the small-world network, but the clustering coefficient (C_p) is high [13]. They allow efficient transmission of information at both the local and global levels [14], and they are also changed in some neuropsychological diseases [15–21]. A recent study has shown that topological clustering was linked with cognitive impairments [22].

There is an increasing interest in brain changes caused by OSAHS. Most studies to date observe brain structural changes in patients. Maceyet [3] found that OSAHS patients had lower FA values of white matter in the anterior corpus callosum, ventral prefrontal, and parietal than healthy controls. Canessa [4] found that OSAHS patients showed impairments in most cognitive areas, which was confirmed by regional homogeneity (Reho) [23] and amplitude of low-frequency fluctuation (ALFF) [24]. However, few studies have addressed changes in the whole brain from the global perspective using small-world parameters. In our study, we adopted the method of graph theory to explore the small-world parameters in whole functional networks for OSAHS patients. This study aims to investigate some possible mechanisms underlying neurological dysfunction in OSAHS patients from a global perspective, which identifies benefits for clinical diagnosis.

2. Methods

2.1. Subjects

A total of 29 OSAHS patients and 26 control adults participated in this research. All subjects signed the informed consent form, and the research was approved by the institutional Ethics Committee, the affiliated Zhong-da Hospital of Southeast University. The participants were recruited from the outpatient division of the otolaryngological department of the affiliated Zhong-da Hospital of Southeast University from November 2014 to January 2016. A total of 29 OSAHS subjects had a definite diagnosis on the basis of the Clinical Diagnostic Interviewing Scale [25]. The inclusion criteria for OSAHS were as follows: only OSAHS and no other sleep disorders; no history of surgery including airway, laryngeal, and pharyngeal; age 20–60 years; no serious cognitive dysfunction; right-handedness; and no MRI contraindications. The inclusion criteria for controls were no OSAHS; gender, age and years of education matched to OSAHS cohort; (c) healthy with no other psychiatric or neurological disorders; and no MRI contraindications. Body mass index (BMI), apnea–hypopnea index (AHI), Oswestry Disability Index (ODI), and Mini Mental State Examination (MMSE) were measured for each patient and control for comparison. All participants included in this research were right-handed. The demographic characteristics of the participants are listed in Table 1.

Table 1
Demographic characteristics of patients.

	OSAHS (n = 29)	Controls (n = 26)	*p*
Age (y)	39.62 ± 9.95	34.46 ± 9.97	6.10×10^{-2}
Gender (M:F)	6:23	8:18	3.92×10^{-1}
EDU (y)	12.67 ± 3.17	13.96 ± 2.58	1.03×10^{-1}
BMI	27.99 ± 4.37	22.16 ± 2.93	8.64×10^{-7}
AHI	33.67 ± 21.75	2.43 ± 1.68	5.45×10^{-8}
ODI	32.07 ± 27.73	0.93 ± 1.03	7.62×10^{-6}
MMSE	28.34 ± 1.65	28.96 ± 1.51	1.70×10^{-1}
ESS	7.69 ± 3.09	4.81 ± 2.61	3.80×10^{-4}
ROCF	35.17 ± 1.00	36.92 ± 0.39	2.08×10^{-3}
DR-ROCF	18.48 ± 7.41	21.89 ± 5.96	2.70×10^{-1}
LM	20.07 ± 7.93	20.69 ± 6.19	8.18×10^{-1}
DR–LM	19.03 ± 8.41	19.77 ± 5.88	7.53×10^{-1}

AHI, apnea–hypopnea index; BMI, body mass index; DR–LM, Delayed Recall trial–logical memory; DR-ROCF, Delayed Recall trial–Rey Osterrieth Complex Figure test; EDU, education; ESS, Epworth Sleepiness Scale; F, female; LM, logical memory; M, male; MMSE, Mini Mental State Examination; ODI, Oswestry Disability Index; ROCF, Rey Osterrieth Complex Figure test.

2.2. MRI data acquisition

All MRI data were collected using a Siemens Verio 3.0 T scanner in the affiliated Zhong-da Hospital of Southeast University at seven days before or after the sleep study. All participants were asked to refrain from consuming alcohol, coffee, etc. on before scanning. A total of 180 Rs-fMRI images from echo-planar imaging (EPI) scans were collected. Scanning sequence and parameters were listed in Table 2.

2.3. Polysomnography

Overnight polysomnography (PSG) was conducted in the hospital. PSG is deemed to be the gold standard in the measurement of breathing during sleep [26]. It is also the method used for diagnosis of sleep-related respiratory disorders.

2.4. Neuropsychological measures

The MMSE was applied to measure the cognitive skills of the subjects. This scale was conducted in an undisturbed environment. Experienced testers evaluated OSAHS patients separately.

2.5. MRI data preprocessing

The preprocessing of MRI data was used by the Data Processing Assistant for Resting-State fMRI (DPARSFA) 2.3. For each run, the top 10 time points of the scanning session were removed. Then the head-motion correction was carried out on the remaining data. The image data were then normalized and spatially smoothed. Finally, filtering was applied to eliminate effects of noise and drift [27].

Table 2
Scanning sequences and parameters.

Sequence	FLAIR	3D T1WI	EPI
TR (ms)	8500	1900	2000
TE (ms)	94	2.48	25
Matrix size	512 × 464	256 × 256	64 × 64
Flip angle (°)	150	9	90
FOV (mm × mm)	240 × 240	256 × 256	240 × 240
Slice	20	176	36
Slice gap (mm)	5	1	4

EPI, echo-planar imaging; FLAIR, fluid attenuated inversion recovery; FOV, field of view; T1W1, T1-weighted images; TE, echo time; TR, repetition time.

2.6. Network construction and graph theoretical analysis of network connection

The brain was divided into 90 anatomical areas of interest to assess the functional connectivity between brain areas, according to the anatomical automatic labeling template (AAL) [28]. A 90 × 90 undirected graph was used to represent the matrix of the functional connectivity network for subjects by calculating the Pearson correlation coefficients between these areas.

To explore the changes in brain networks, all the correlation matrices were thresholded, where edges stand for undirected connections and nodes stand for brain regions.

Several parameters are used to summarize the properties of OSAHS and matched groups, including clustering coefficient (C_p), shortest path length (L_p), global efficiency (E_{global}), and local efficiency (E_{local}) [29].

- C_p clustering of nodes, implying the networks ability of local information transmitting, defined as

$$C(i) = \frac{2E_i}{K_i(K_i - 1)}. \quad (1)$$

- L_p minimum length between two nodes, which is important to the transmission of information in network, defined as

$$L = \frac{1}{N(N-1)} \sum_{i,j \in V, i \neq j} l_{ij}. \quad (2)$$

- E_{local} ability measurement of local information transmitting in the network, defined as

$$E(i) = \frac{1}{N_{G_i}(N_{G_i} - 1)} \sum_{j \neq k \in G_i} \frac{1}{l_{j,k}}, \quad (3)$$

$$E_{local} = \frac{1}{N} \sum_{i \in V} E(i). \quad (4)$$

- E_{global} measurement of the ability of global information transmitting in the network together with L_p, defined as

$$E_{global} = \frac{1}{N(N-1)} \sum_{i,j \in V, i \neq j} \frac{1}{l_{i,j}}. \quad (5)$$

A group of additional small-world network parameters were defined [30,31] to further explain the phenomena, including the following: γ, the ratio of the clustering coefficients in real and random network; λ, the ratio of the path length in real and random network; and σ, the scalar measurement of small-world network. Their relationships with the clustering coefficients and the path lengths are

$$\gamma = \frac{C_p}{C_r}, \quad (6)$$

$$\lambda = \frac{L_p}{L_r}, \quad (7)$$

where C_p and C_r denote research networks and random networks respectively from the average clustering coefficients, and L_p and L_r represent research networks and random networks respectively from the average path length. In addition, there is also

$$\sigma = \frac{\gamma}{\lambda}. \quad (8)$$

These small-world property calculations are targeted toward the influence of random networks. The parameters γ and λ reflect the change in the real brain network to the random network or the regular network [32].

2.7. Statistical analysis

In our present study, an analysis of covariance (ANCOVA) was used to eliminate the potential influences of the census variables including age, educational level, investigate changes in the topological properties (L_p and C_p), and results of neuropsychological tests. We constructed brain functional networks in sparsity between 0.1 and 0.5, with an interval of 0.01. We first verified that the small-world parameters (E_{global}, E_{local}) followed a normal distribution. Then the global metrics (E_{global} and E_{local}) were compared to explore the changes in the network in the two groups through a two-sample analysis of variance (statistical threshold of $p < 0.05$).

3. Results

3.1. Demographics

No statistical differences were observed between groups in age ($p = 0.061$), gender ($p = 0.392$), or education level ($p = 0.103$). At the same time, BMI, AHI, and ODI increased significantly in the OSAHS group over the control ($p < 0.05$), but no significant differences were observed with the MMSE ($p = 0.170$). The p values for BMI, AHI, ODI, and MMSE are given in Table 3.

3.2. Small-world networks

The linear graph of the control groups and OSAHS shows that $\gamma > 1$, $\lambda \approx 1$, $\sigma > 1$, suggesting that the functional brain network pertains to the small-world properties in both groups (Fig. 1).

3.3. Analysis of small-world properties between the two groups

The properties of the small-world network in the two groups were different from the linear graph. For the sparsity of 0.1–0.2, seven topological metrics parameters of small-world between two groups were calculated, among which C_p, E_{local}, and E_{global} showed positive correlation with sparsity, whereas L_p, γ, λ, and σ showed negative correlation with sparsity. Meanwhile, C_p, E_{local}, and E_{global} of OSAHS subjects decreased significantly compared to those in the control group ($p < 0.05$), whereas L_p was increased compared to that in the control group ($p < 0.05$). The linear graph of seven parameters is given in Fig. 1.

Table 3
Differences in BMI, AHI, ODI, and MMSE between the two groups.

	OSAHS (n = 29)	Controls (n = 26)	p	T
BMI	28.0 ± 4.4	22.2 ± 2.9	0.000	5.749
AHI	33.8 ± 21.8	2.4 ± 1.7	0.000	7.706
ODI	32.1 ± 27.7	0.9 ± 1.0	0.000	6.041
MMSE	28.3 ± 1.7	29.0 ± 1.5	0.156	−1.439

AHI, apnea–hypopnea index; BMI, body mass index; MMSE, Mini Mental State Examination; ODI, oxygen desaturation index.

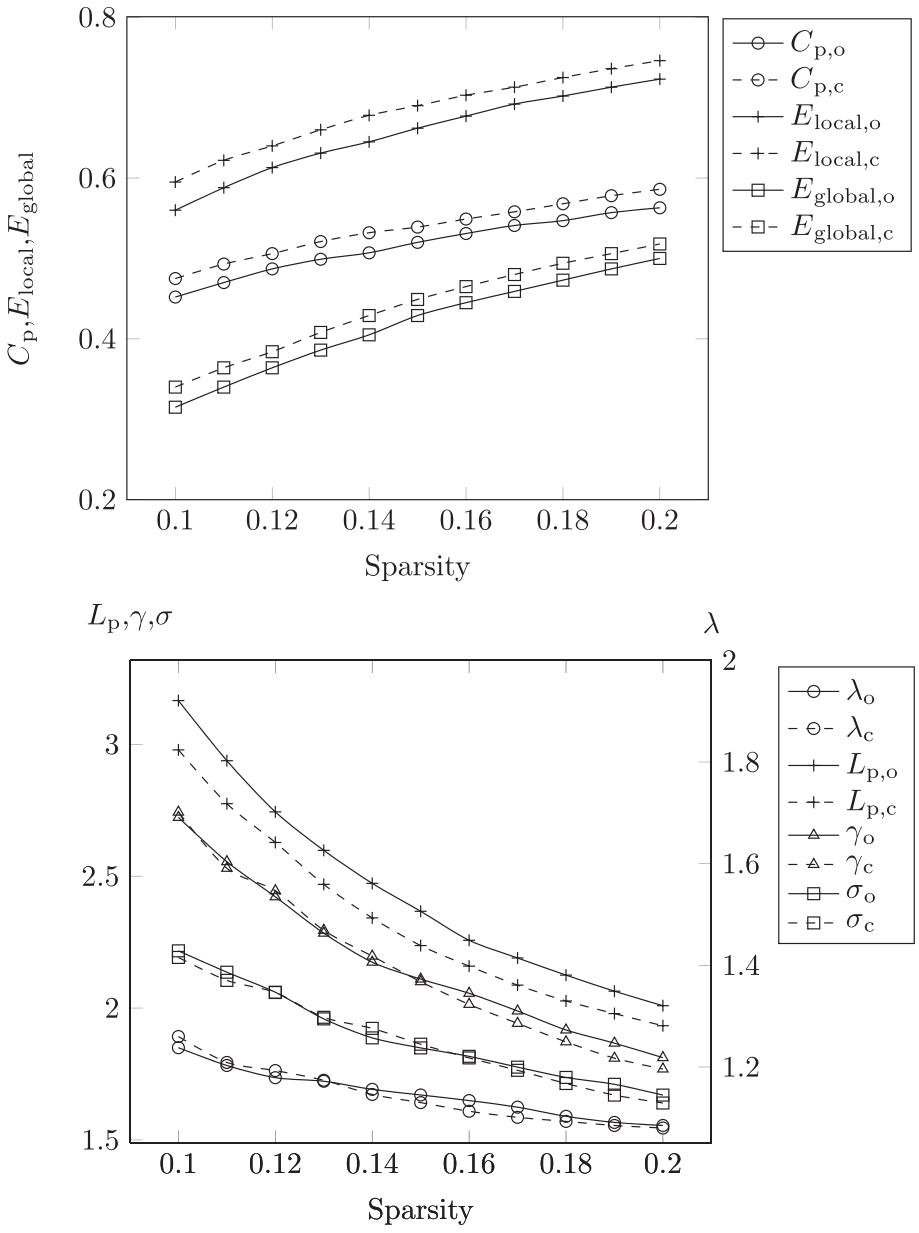

Fig. 1. Linear graphs of the 7 small-world parameters for controls (with footnote c) and OSAHS (with footnote o) groups, including cluster coefficient C_p, the global metrics E_{local} and E_{global}, shortest path length L_p, the ratio of the clustering coefficients in real and random network γ, the ratio of the path length in real and random network λ, and the scalar measurement of small-world network σ, for the sparsity of 0.1 to 0.2.

4. Discussion

The incidence of OSA is about 49% in adults [33,34]; OSA affects 3% to 7% of adult men and 2% to 5% of adult women in the general population [33–35]. Studies have shown that the function of important organs was seriously affected, including brain damage [37]. Patients also lost coordination, with atonia of the upper airway muscles and airway collapse [38]. Most patients with OSAHS have a certain degree of cognitive dysfunction, executive dysfunction, and emotional disorders, but the mechanism of its inherent neurological dysfunction is unclear.

Regions of the brain not only have relatively independent functions but also have networks of functional connection. Each interaction between different brain areas supports the function of the brain activity [39]. Graph theory shows the perspective of information transmitted in the network. The brain's functional network can be treated as an aggregate containing nodes and edges [40,41]. If the brain integrity can be reflected by whole-brain network topological properties, these properties can be set in the network nodes to represent local performance. Nodes represent different brain regions, and the edge is the connection between the nodes [42].

Functional networks of the brain show efficient small-world characteristics; these properties are influenced by neurological biological factors. Studies have shown that differences in these small-world measures can be seen between case groups and control groups in functional connectivity or effective connectivity [43].

In this study, the OSAHS groups with the result $\gamma, \sigma > 1$ and $\lambda \approx 1$ suggests that the functional network satisfied the efficient properties in the threshold 0.1 to 0.2, similar to other diseases [15,21].

Even through the conditions for small-worldness did exist, some properties of the network had changed.

Within the scope of the threshold 0.1–0.2, C_p showed a tendency to increase, as well as E_{global}, E_{local}, and L_p (Fig. 1). It is worth noting that L_p was longer in the patient group compared to that in the controls in the range of each sparsity, whereas C_p was decreased ($p < 0.05$). Across the sparsity levels of the threshold (0.1–0.2), E_{global} and E_{local} decreased in OSAHS patients compared to the control group ($p < 0.05$). However, γ, σ, and λ did not show statistical significance differences across the groups.

As C_p shows the density of cluster groups, its reduction may reflect the damage to brain network function, as well as inefficiency of information transmission [44]. L_p may relate to the process of cognitive function [45,46]. The shorter that L_p becomes, the more efficient and rapid information is transmitted in the whole brain. By contrast, the long path length may imply disrupted neuronal integration between the regions. E_{global} measures the ability of global information transmission in the network, together with L_p. The shortest path length is inversely proportional to E_{global}; the longer is L_p, the lower E_{global} and the slower the transmission of information in the network.

Through our research, we have shown that small-world properties were significantly different in OSAHS group compared to those of the control group. The majority of the threshold values the L_p of OSAHS group was significantly longer than controls ($p < 0.05$); the corresponding E_{global} was lower, and the measurement of efficiency may be superior to traditional measurement of C_p and L_p [47]. These findings suggest that effective integrity and global information propagation had been disrupted, which influenced the rate of information transmission, and implied the disconnection or uneconomical nature of the graph theory. However, the exact reason is still unclear, and one possible reason can be age. Studies have found that the properties of the networks will change along with growth, as well as with acquired learning [48], gender [49], disease, and damage to cognition [16,50,51]. The human brain functional networks constructed by different brain atlases all satisfied the small-world conditions, but each of its parameter properties had significant differences between groups, including the network, the shortest path length (L_p), cluster coefficient (C_p), E_{global} and E_{local}, which is consistent with the results in this study.

In brief, the small-world structure reflects the balance of brain network at both the global and local levels. Any factor that causes abnormal changes in the brain restructures the network, which is not the ideal state, either transformation to the random networks or the regular networks. Our study findings suggested that the change to the random networks of brain networks of OSAHS patients may reflect a kind of abnormal network structure.

In this study, BMI, AHI, and ODI values in the OSAHS group were significantly higher than in the controls ($p < 0.05$). The obvious differences in the three indicators suggest that the function of the OSAHS group's brain have changed together with properties of whole-brain functional networks of the small world. Research has shown that reduced cognitive ability is associated with L_p. Thus, changes in the small-world parameters of the brain functional network in the OSAHS group may relate to cognitive dysfunction. The MMSE did not show obvious differences between the two groups ($p > 0.05$), suggesting that MRI maybe more sensitive than MMSE in the early detection and diagnosis of cognitive impairment in patients with OSAHS.

At present, few resting-state functional MRI studies have been conducted in OSAHS patients; there is relatively little study about whole-brain functional network in OSAHS patients. Several studies using magnetic resonance spectroscopy have demonstrated significant metabolic changes in OSAHS [5,52] and changing resting-state brain activity [53]. The changes in small-world topological properties in OSAHS patients may be caused by brain dysfunction, and the topological properties of change also can reflect damage to the brain function. MRI has advantages in the early diagnosis of OSAHS. At the same time, changes in the brain functional network may be helpful in clinical diagnosis. Therefore, the study of properties of brain functional network in OSAHS patients can not only provide a new perspective for the pathogenesis of OSAHS, but can also be helpful for deepening our understanding of this disease.

Limitations of our research include the relatively small cohort size, and the normalization accuracy of postprocessing. The p value of age was at the limit of the statistical threshold, which seems to indicate a lack of rigor; although significant group differences had been found between groups, the limited number of subjects may have restricted the ability to show more group differences. We did not conduct a longitudinal follow-up study for OSHAS patients before and after treatment, which would contrast the dynamic changes in brain functional networks when the structure and function have changed [54]. In future research, the differences in brain functional networks between males and females and between mild-to-moderate and severely ill patients will be explored to verify our results.

5. Conclusion

Both OSAHS patients and healthy controls exhibited small-world properties in functional networks; however, a subset of these small-world properties in OSAHS patients were different, including node clustering, local information, and minimum node length.

These changes will not only provide a new perspective on the pathophysiological mechanism of OSAHS but will also be helpful for understanding this disease in terms of whole-brain functional networks. MRI provides an advantage in the early diagnosis of OSAHS, and the measurement of changes in the brain functional network may be helpful for clinical diagnosis.

Acknowledgments

The study was supported by the project of the Women's and Children's Health of Jiangsu Province (Grant No F201554), Technological Development of Nanjing City (2015sc511023), Six Talent Peaks Project in Jiangsu Province (WSN-192), China and Technological Development of Nanjing Medical University (2016NJMU089), China.

Conflict of interest

The ICMJE Uniform Disclosure Form for Potential Conflicts of Interest associated with this article can be viewed by clicking on the following link: https://doi.org/10.1016/j.sleep.2018.08.037.

References

[1] Vecchierini MF, Attali V, Collet JM, et al. A custom-made mandibular repositioning device for obstructive sleep apnoea-hypopnoea syndrome: the ORCADES study. Sleep Med 2016;19:131–40.
[2] Sajkov D, McEvoy RD. Obstructive sleep apnea and pulmonary hypertension. Prog Cardiovasc Dis 2009;51:363–70.
[3] Macey PM, Kumar R, Woo MA, et al. Brain structural changes in obstructive sleep apnea. Sleep 2008;31:967–77.
[4] Canessa N, Castronovo V, Cappa SF, et al. Obstructive sleep apnea: brain structural changes and neurocognitive function before and after treatment. Am J Respir Crit Care Med 2011;183:1419–26.

[5] Algin O, Gokalp G, Ocakoglu G, et al. Neurochemical-structural changes evaluation of brain in patients with obstructive sleep apnea syndrome. Eur J Radiol 2012;81:491–5.
[6] Sarchielli P, Presciutti O, Alberti A, et al. 1h Magnetic resonance spectroscopy study in patients with obstructive sleep apnea. Eur J Neurol 2008;15:1058–64.
[7] Zhang X, Ma L, Li S, et al. A functional MRI evaluation of frontal dysfunction in patients with severe obstructive sleep apnea. Sleep Med 2011;12:335–40.
[8] Sweet LH, Jerskey BA, Aloia MS. Default network response to a working memory challenge after withdrawal of continuous positive airway pressure treatment for obstructive sleep apnea. Brain Imaging Behav 2010;4:155–63.
[9] George CF. Sleep. 5: driving and automobile crashes in patients with obstructive sleep apnoea/hypopnoea syndrome. Thorax 2004;59:804–7.
[10] Riha RL. Diagnostic approaches to respiratory sleep disorders. J Thorac Dis 2015;7:1373–84.
[11] Kim YC, Lebel RM, Wu Z, et al. Real-time 3D magnetic resonance imaging of the pharyngeal airway in sleep apnea. Magn Reson Med 2014;71:1501–10.
[12] Sporns O. Structure and function of complex brain networks. Dialogues Clin Neurosci 2013;15:247–62.
[13] Phillips DJ, McGlaughlin A, Ruth D, et al. Alzheimer's disease neuroimaging. Graph theoretic analysis of structural connectivity across the spectrum of Alzheimer's disease: the importance of graph creation methods. Neuroimage Clin 2015;7:377–90.
[14] Bassett DS, Bullmore E. Small-world brain networks. Neuroscientist 2006;12:512–23.
[15] Li W, Li Y, Zhu W, et al. Changes in brain functional network connectivity after stroke. Neural Regen Res 2014;9:51–60.
[16] Baek K, Morris LS, Kundu P, et al. Disrupted resting-state brain network properties in obesity: decreased global and putaminal cortico-striatal network efficiency. Psychol Med 2017;47:585–96.
[17] Zhang GY, Yang M, Liu B, et al. Changes in the default mode networks of individuals with long-term unilateral sensorineural hearing loss. Neuroscience 2015;285:333–42.
[18] Huang W, Huang D, Chen Z, et al. Alterations in the functional connectivity of a verbal working memory-related brain network in patients with left temporal lobe epilepsy. Neurosci Lett 2015;602:6–11.
[19] Zhang Z, Zheng H, Liang K, et al. Functional degeneration in dorsal and ventral attention systems in amnestic mild cognitive impairment and Alzheimer's disease: an fMRI study. Neurosci Lett 2015;585:160–5.
[20] Zhang J, Li Y, Chen H, et al. An investigation of the differences and similarities between generated small-world networks for right- and left-hand motor imageries. Sci Rep 2016;6:36562.
[21] Xu H, Ding S, Hu X, et al. Reduced efficiency of functional brain network underlying intellectual decline in patients with low-grade glioma. Neurosci Lett 2013;543:27–31.
[22] Giessing C, Thiel CM, Alexander-Bloch AF, et al. Human brain functional network changes associated with enhanced and impaired attentional task performance. J Neurosci 2013;33:5903–14.
[23] Santarnecchi E, Sicilia I, Richiardi J, et al. Altered cortical and subcortical local coherence in obstructive sleep apnea: a functional magnetic resonance imaging study. J Sleep Res 2013;22:337–47.
[24] Li HJ, X. Dai XJ, Gong HH, et al. Aberrant spontaneous low-frequency brain activity in male patients with severe obstructive sleep apnea revealed by resting-state functional MRI. Neuropsychiatr Dis Treat 2015;11:207–14.
[25] Ito E, Inoue Y. The international classification of sleep disorders, third edition. American Academy of Sleep Medicine. Includes bibliographies and index [in Japanese]. Nihon Rinsho 2015;73:916–23.
[26] Gasparini G, Vicini C, De Benedetto M, et al. Diagnostic accuracy of obstructive airway adult test for diagnosis of obstructive sleep apnea. Biomed Res Int 2015:915185. https://doi.org/10.1155/2015/5185.
[27] Yu Y, Zhou X, Wang H, et al. Small-world brain network and dynamic functional distribution in patients with subcortical vascular cognitive impairment. PLoS One 2015;10, e0131893.
[28] Tzourio-Mazoyer N, Landeau B, Papathanassiou D, et al. Automated anatomical labeling of activations in SPM using a macroscopic anatomical parcellation of the MNI MRI single-subject brain. Neuroimage 2002;15:273–89.
[29] Latora V, Marchiori M. Efficient behavior of small-world networks. Phys Rev Lett 2001;87:198701.
[30] Watts DJ, Strogatz SH. Collective dynamics of 'small-world' networks. Nature 1998;393:440–2.
[31] Humphries MD, Gurney K, Prescott TJ. The brainstem reticular for- mation is a small-world, not scale-free, network. Proc Biol Sci 2006;273:503–11.
[32] Jiang G, Wen X, Qiu Y, et al. Disrupted topological organization in whole-brain functional networks of heroin-dependent individuals: a resting-state fMRI study. PLoS One 2013;8, e82715.
[33] Feng J, Chen BY. Prevalence and incidence of hypertension in obstructive sleep apnea patients and the relationship between obstructive sleep apnea and its confounders. Chin Med J (Engl) 2009;122:1464–8.
[34] Feng J, Wu Q, Zhang D, et al. Hippocampal impairments are associated with intermittent hypoxia of obstructive sleep apnea. Chin Med J (Engl) 2012;125:696–701.
[35] Park JG, Ramar K, Olson EJ. Updates on definition, consequences, and management of obstructive sleep apnea. Mayo Clin Proc 2011;86:549–54. quiz 554–5.
[37] Morrell MJ, McRobbie DW, Quest RA, et al. Changes in brain morphology associated with obstructive sleep apnea. Sleep Med 2003;4:451–4.
[38] Yadav SK, Kumar R, Macey PM, et al. Regional cerebral blood flow alterations in obstructive sleep apnea. Neurosci Lett 2013;555:159–64.
[39] Bullmore E, Sporns O. The economy of brain network organization. Nat Rev Neurosci 2012;13:336–49.
[40] Rubinov M, Sporns O. Complex network measures of brain connectivity: uses and interpretations. Neuroimage 2010;52:1059–69.
[41] Wang JH, Zuo XN, Gohel S, et al. Graph theoretical analysis of functional brain networks: test-retest evaluation on short- and long-term resting-state functional MRI data. PLoS One 2011;6, e21976.
[42] Bai F, Shu N, Yuan Y, et al. Topologically convergent and divergent structural connectivity patterns between patients with remitted geriatric depression and amnestic mild cognitive impairment. J Neurosci 2012;32:4307–18.
[43] Horwitz B, Hwang C, Alstott J. Interpreting the effects of altered brain anatomical connectivity on fMRI functional connectivity: a role for computational neural modelling. Front Hum Neurosci 2013;7:649.
[44] van den Heuvel MP, Stam CJ, Boersma M, et al. Small-world and scale-free organization of voxel-based resting-state functional connectivity in the human brain. Neuroimage 2008;43:528–39.
[45] Zuo XN, Ehmke R, Mennes M, et al. Network centrality in the human functional connectome. Cereb Cortex 2012;22:1862–75.
[46] Wee CY, Zhao Z, Yap PT, et al. Disrupted brain functional network in internet addiction disorder: a resting-state functional magnetic resonance imaging study. PLoS One 2014;9, e107306.
[47] Wang L, Zhu C, He Y, et al. Altered small-world brain functional networks in children with attention-deficit/hyperactivity disorder. Hum Brain Mapp 2009;30:638–49.
[48] Gong G, Rosa-Neto P, Carbonell P, et al. Age- and gender-related differences in the cortical anatomical network. J Neurosci 2009;29:15684–93.
[49] Micheloyannis S, Pachou E, Stam CJ, et al. Using graph theoretical analysis of multi channel EEG to evaluate the neural efficiency hypothesis. Neurosci Lett 2006;402:273–7.
[50] Batalle D, Munoz-Moreno E, Tornador C, et al. Altered resting-state whole-brain functional networks of neonates with intrauterine growth restriction. Cortex 2016;77:119–31.
[51] Sanz-Arigita EJ, Schoonheim MM, Damoiseaux JS, et al. Loss of 'small-world' networks in Alzheimer's disease: graph analysis of fMRI resting-state functional connectivity. PLoS One 2010;5, e13788.
[52] Alchanatis M, Deligiorgis N, Zias N, et al. Frontal brain lobe impairment in obstructive sleep apnoea: a proton MR spectroscopy study. Eur Respir J 2004;24:980–6.
[53] Peng DC, Dai XJ, Gong HH, et al. Altered intrinsic regional brain activity in male patients with severe obstructive sleep apnea: a resting-state functional magnetic resonance imaging study. Neuropsychiatr Dis Treat 2013;10:1819–26.
[54] O'Donoghue FJ, Wellard RM, Rochford PD, et al. Magnetic resonance spectroscopy and neurocognitive dysfunction in obstructive sleep apnea before and after CPAP treatment. Sleep 2012;35:41–8.